Wiley Online Library
Early View publication on www.wileyonlinelibrary.com
(issue and page numbers not yet assigned;
citable using Digital Object Identifier – DOI)

Phys. Status Solidi A, 1700238 (2017) / DOI 10.1002/pssa.201700238

physica status solidi a
www.pss-a.com
applications and materials science

Deep carrier traps in as grown isotopically pure ^{28}Si FZ crystal

Teimuraz Mchedlidze*[,1], Jörg Weber[1], Nikolay V. Abrosimov[2], and Helge Riemann[2]

[1] Technische Universität Dresden, Haekelstr. 3, 01062 Dresden, Germany
[2] Leibniz Institute for Crystal Growth, Max Born Str. 2, D-12489 Berlin, Germany

Received 3 April 2017, revised 19 April 2017, accepted 19 April 2017
Published online 31 May 2017

Keywords charge carrier traps, crystals, deep level transient spectroscopy, defects, float-zone growth, silicon

* Corresponding author: e-mail teimuraz.mtchedlidze@physik.tu-dresden.de, Phone: +49-351-463 37227, Fax: +49-351-463 37060

We studied a distribution of dopants and carrier traps in the FZ grown ^{28}Si crystal. Samples cut-out from various parts of an as-grown crystal were analysed by deep level transient spectroscopy (DLTS) and photoluminescence (PL). Several traps were detected at the concentration level of $\sim 10^{10}$ cm^{-3} by DLTS. Careful analyses of the obtained signals allow attributing the related traps to agglomerates of intrinsic defects. A correlation of the trap concentration to the phosphorus doping, detected by PL and confirmed by electric measurements was also observed. A possible attribution of the traps to the previously reported defects will be discussed.

1 Introduction Recently, silicon crystals grown under the enrichment of single isotopes (e.g. ^{28}Si) have attracted a large amount of interest because of the combination of high crystal quality and the unique thermal, electrical, magnetic and optical properties. The variation in the isotope content in the lattice influences the average atomic mass, affecting the phonon frequencies, the band gap and spectral line widths. The absence of atoms with a nuclear magnetic moment (i.e. ^{29}Si) makes the material 'magnetically pure', which may have applications in quantum information technologies [1]. Isotopically pure and perfect ^{28}Si crystal is regarded as a possible source for the creation of a novel natural kilogram mass unit standard, which will replace the present definition of the kilogram (project 'Avogadro' at seq.) [2]. The last step in the technological process of material preparation is the growth of the dislocation-free ^{28}Si single crystal with the total impurity concentrations smaller than 10^{15} cm^{-3} that should be used for the accurate determination of the Avogadro constant based on the measurement of ^{28}Si spheres. High crystal perfection and high purity are necessary to achieve the measuring uncertainty towards the 10^{-9} range before the definition of the kilogram can be changed. In depth characterisation of the as-grown material is also necessary to enable the specified future applications.

From the start of the fabrication of ^{28}Si-enriched crystals (see Ref. [1] for details), the material was investigated with various techniques and methods. Spin resonance studies (see e.g. Ref. [3] and references therein), infrared absorption spectroscopy studies (see Ref. [4] and references therein), and photoluminescence (PL) studies (see Ref. [5] and references therein) have revealed many unique properties of the material itself. In addition, the material improved our knowledge about defect properties in Si. To the best of our knowledge, deep carrier traps were not yet investigated in the as-grown crystals using a deep level transient spectroscopy (DLTS). On the other hand, the low level of dopant concentrations ($\sim 10^{13}$ cm^{-3}) and low level of oxygen and carbon atoms ($\leq 10^{15}$ cm^{-3}) may substantially change the interaction of vacancies and interstitials during the crystal growth/cooling and affect the formation of as-grown defects. Moreover, the low doping level gives the possibility of probing impurity concentrations down to the $\sim 10^{9}$ cm^{-3} level.

2 Samples and experimental General details of FZ-^{28}Si crystal growth can be found in Ref. [2]. Carbon concentration in the starting polycrystalline rod applied for the growth of present crystal was slightly over the upper limit of the desired concentration level ($<2 \times 10^{15}$ cm^{-3}), and therefore, five purification runs were carried out before

the growth of the end crystal. Two of the runs were done in a vacuum to avoid oxygen incorporation. As a result, the oxygen concentration over the whole crystal length was less than 2×10^{14} cm^{-3} and carbon concentration changed from less than 2×10^{14} cm^{-3} at the top to about 3×10^{15} cm^{-3} at the tail, according to the segregation behaviour during FZ crystal growth. The dislocation free ^{28}Si end crystal, 100.3 mm in diameter, was grown in Ar atmosphere with small admixture of nitrogen.

Samples for DLTS analyses were cut-out from the top, middle and tail parts of the crystal. The sample labelled N516 was cut-out at ~20% of length from the top part of the crystal, near to the rim. The sample labelled Q23 was cut-out from the middle part of the crystal (at ~48% of the length), near to the rim. The samples labelled V732 and V737 were cut out from the tail part of the crystal, at ~86% of the length. The V737 sample was cut-out from a location near to the rim of the crystal and V732 from a location close to the center of the crystal. The size of all samples was close to $4 \times 4 \times 0.5$ cm^3.

All samples were polished mechanically by SiC paste and chemically by HF + HNO_3 (1:5) solution (3 min at RT). The polishing was finished by a dip in HF + H_2O (1:10) solution for 30 s at RT. All samples showed n-type conductivity and therefore, a 100 nm thick Au film was thermally evaporated on the surface of the samples for Schottky contact formation. The diameter of the contacts was 2 mm. For the Ohmic contacts InGa eutectic was scratched in at the sample backside.

Standard room temperature capacitance-voltage (*CV*) measurements on the Schottky diodes were performed with a PC-controlled HP capacitance meter to determine the doping level. DLTS measurements were performed by the means of a standard lock-in system, working at the capacitance testing frequency of 1 MHz. The principles of the method and the system were previously described [6]. Cooling of a sample was done by immersion in a dewar with liquid He and a temperature controller maintained the necessary temperature in the range of 35–300 K. Carrier-trap parameters, their concentrations, dependences of the DLTS signals on the excitation pulse length were measured using standard DLTS measurement and data processing procedures [6]. Measurements of depth distribution for the traps and high-resolution energy level position measurements were done using the Laplace DLTS (LDLTS) technique [7].

To establish the origin of the doping and conductivity type, low temperature PL measurements were performed on the same samples, which were used for the DLTS measurements. The details of the PL measurements were similar to those presented in Ref. [8].

3 Results and discussion All investigated samples showed n-type conductivity. PL measurements were conducted to confirm the prevailing content of phosphorus (P) donors and to check the compensation by boron (B) acceptors. We use the ratio of the bound exciton to free exciton intensities to determine the doping concentrations. The intensities were correlated with the dopant concentrations by using our own calibration curves and those from the literature [9, 10]. Differences in the concentrations due to the different calibration curves were in the 10% range. In quantitative agreement with the *CV*-profiles, an increase of the P concentration from the top to the bottom part of the ingot was detected. This effect can be expected after multiple purification runs. The boron concentration remains constant in that direction and varies locally from 2 to 3×10^{12} cm^{-3}. Only in sample (V732) the PL measurements did reveal the presence of the D-band luminescence, previously attributed to a recombination at dislocations.

Four DLTS peaks were detected in sample V737. The spectrum recorded for a sampling time $\tau_p = 50$ ms and a filling pulse length $t_p = 0.5$ ms is presented in Fig. 1. The numbers in the labels of the traps indicate the temperature for the peak maximum, "E" stands for electron traps. With the standard procedure of DLTS measurements at various τ_p (from 11 to 256 ms) and an Arrhenius analyses for the peak maximum positions (see Fig. 2) the energy levels were determined. The level positions and the respective trap concentrations in the different samples are presented in Table 1. Trap concentrations were calculated from the amplitudes of the peaks [6].

A fitting of the experimental spectra was performed by using the model for point-like defects or that for extended defects with the parameters from the Arrhenius analysis [11]. As seen from Fig. 1, fitting of the experimental spectrum using the point-like defect model is poor, especially for the peak E206 and in less extent to the peaks E117 and E88. The reason for the poor fitting can be either an overlap of several DLTS peaks with similar/close trap parameters or an extended structure of defects. The LDLTS measurements

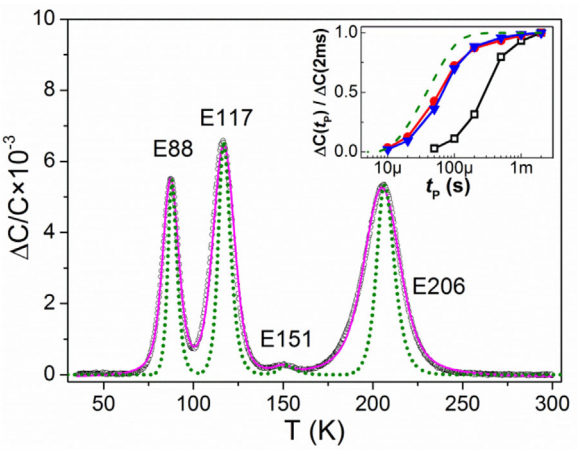

Figure 1 DLTS spectrum (open circles) detected from sample V737 for $\tau_p = 50$ ms and $t_p = 0.5$ ms. Filled dots present fit of the spectrum with point-like defect transient model, solid curve presents fit using model for extended defects (see text). In the inset – $\Delta C(t_P)$ dependencies for the signals normalised on their amplitude for $t_P = 2$ ms: open squares – E206, circles – E117 and triangles – E88; dashed curve presents a typical dependence for point-like defects.

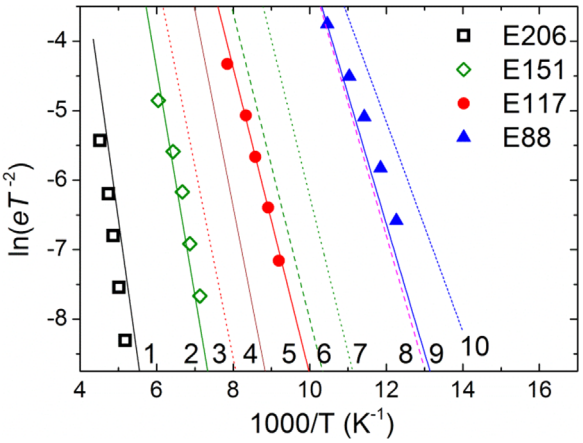

Figure 2 Arrhenius plots for the detected traps (closed symbols) and previously reported signatures of the defects: 1, 3, 7 – dislocations [12, 13]; 2, 5, 10 – defects in nitrogen doped as-grown Fz-Si crystals [14]; 4, 8 – vacancy complexes [15]; 6, 9 – interstitial complexes and rod-like defects [16, 17] (see the text for more details).

did not reveal the presence of multiple traps related to the peaks, therefore the overlap of multiple peaks was not a case. On the other hand, measurements of the peak amplitude dependencies on the filling pulse duration (for $t_p \leq 2$ ms, see inset in Fig. 1) showed no saturation with the pulse length, indicating an extended structure of the related traps.

In the bulk of the individual samples traps were distributed homogeneously with depth within an accuracy of ~15%. In contrast to that, concentration of the traps strongly varied from sample to sample with the ultimate maximum for the samples cut-out from the rim location at the tail of the crystal (i.e. sample V737). Indeed, the V737 and V732 samples were cut-out from the crystal region where back-gliding dislocations appeared during post growth crystal cooling.

The extremely low level of trap concentrations ($5 \times 10^9 \div 5 \times 10^{11}$ cm^{-3}) makes it difficult to select the origin of the DLTS peaks. A short list of possible candidates contains metal contaminants, hydrogen, carbon, oxygen-related defects, intrinsic defect complexes or structural defects. Fortunately, many candidates can be sorted out from the start due to extended structure of the traps responsible for the peaks. It should be noted that due to the very small concentrations of impurities (much below the solubility limits of most elements in silicon), formation of precipitates from impurity atoms also can be neglected. The absence of depth-dependence excludes defects possibly formed during sample preparation for the measurements, i.e. hydrogen-related centers formed due to the etching. Therefore, the remaining possibilities include structural defects, i.e. dislocations and complexes of intrinsic defects (vacancies and interstitials).

Table 1 Energy level positions and concentrations of the traps in various samples.

		trap concentration ($\times 10^{10}$ cm^{-3})			
trap	E_C-E_t (eV)	V373	V732	Q23	N516
E206	0.38 ± 0.02	47	6.4	1.04	0.22
E151	0.23 ± 0.02	2	0.6	<0.5	<0.06
E117	0.18 ± 0.01	53	4.2	<0.4	<0.1
E88	0.14 ± 0.01	44	3.7	2.85	0.62

Using the database for the defects detected in Si by DLTS [18] and the references therein, several possibilities for the origin of the peaks were checked. The Arrhenius fits for the closest matches are shown in Fig. 2 by lines with numbers.

The E206 peak, with maximal amplitude in V737 sample, probably can be attributed to dislocation-related traps. Line 1 in Fig. 2 presents a signature of the so-called DE2 trap detected in plastically deformed n-type Si after annealing of the sample at $T > 850$ °C [12]. Two facts make such attribution probable. First, that the presence of back-gliding dislocations on the crystal surface was observed after the growth near the position of the sample V737. And second, the DE2 trap is the only one which survives high temperature treatments after plastic deformation [12]. As seen from Fig. 2, the other dislocation-related traps, i.e. DE1 [12] and DA [13] do not match the signatures detected in our samples. The same holds for other traps, which were attributed to dislocations (see Refs. [12, 13] and references therein). This gives us possibility to suppose that the back-gliding dislocations were formed at $T_{cooling} > 850$ °C. It should be noted that for extended defects it is not possible to estimate the related defect density from the DLTS peak amplitude, due to the possible multiple capture/excitation processes of the carriers to/from the same trap during the single pulse [11, 12]. Therefore the trap concentration for E206 in Table 1, estimated from the DLTS signal amplitude, may only roughly correlate with the actual dislocation density in the material.

Parameters of other traps detected in our samples, i.e. E151, E117 and E88 are very close to the NA, NB and N013 traps detected in as-grown FZ-Si crystals fabricated under nitrogen atmosphere [14]. Since the present crystal was also grown in the atmosphere containing nitrogen, appearance of these traps could be expected. Unfortunately, the authors [14] do not give further identification of the origin for the traps, except an attribution of NA and NB to nitrogen-related defects. For N013 no correlation with the nitrogen pressure was found in Ref. [14].

Examples of several vacancy complexes (with the parameters close to those detected in our study) are also presented in Fig. 2. The closest match is VO complex (line 8, A-center [15]). The problem with this identification is that most small vacancy complexes anneal out below $T < 450$ °C [19] and moreover, these small complexes cannot be attributed to extended defects. As for the large vacancy complexes, it is widely accepted [20], that their

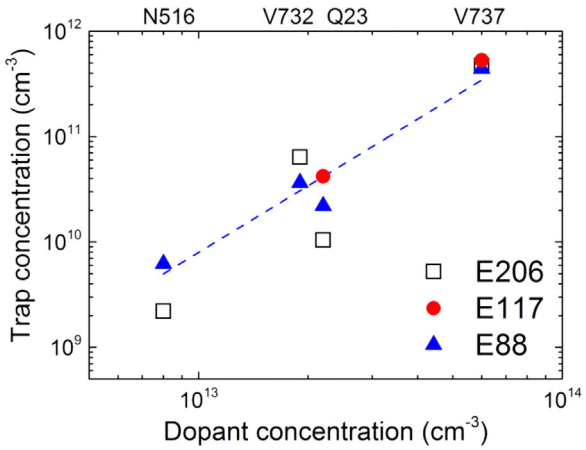

Figure 3 Correlation between doping level and trap concentration in the samples. Dotted line presents least square fit for E88 trap data.

electrical activity can be related only to the decoration with metal atoms, not found in this crystal.

Interstitial atoms in silicon can form extended complexes of various sizes starting from I2 and finishing with so-called rod-like defects (RLD, see Ref. [19] and references therein). Small interstitial complexes are annealed at $T < 600\,^{\circ}$C, but RLDs are more stable. Their DLTS signatures vary with their size [16, 17]. Two of the RLD signatures, closest to the detected traps are presented in Fig. 2 by lines 6 and 9.

A correlation of the concentrations of the E88 and E117 levels with the phosphorus doping in the samples is also detected (see Fig. 3). Note that, correlation of the E206 traps with the doping level is not that obvious. The nearly two times difference in donor concentration between the V737 and V732 samples detected by *CV* measurements is in agreement with that observed and calculated radial distribution of P for the similar growth conditions of FZ Si [21].

Based on the above-mentioned references and the obtained results, we propose that E88 and E117 traps are related to some agglomerates of interstitials formed at the late stage of cooling of the crystal. While E206 may be attributed to dislocation-related traps. The similarity of the traps detected in the present work with those from Ref. [14] may help in identifying an origin for the defects in the present study. Indeed, nitrogen is supposed to be an effective vacancy-trap [22], causing significant decrease of sizes for in-grown voids in the Cz-Si crystals [23]. A deficit of vacancies may lead to an increase of the self-interstitial concentration and initiate a formation of their complexes. Since oxygen, another strong trap for vacancies, is at very low concentrations in the present crystal ($<2 \times 10^{14}\,\mathrm{cm}^{-3}$), phosphorus may act similarly to nitrogen and might cause the observed correlation of the trap concentrations with the doping level.

The strongly non-linear dependence of the trap concentrations from the P concentrations (see Fig. 3, the less square fit shown by dotted line corresponds to $C_{\mathrm{trap}} \sim C_{\mathrm{P}}^{2}$) suggests that more than one interstitial is needed to form the trap centres. This fact also agrees with the extended structure of the traps.

4 Summary Carrier traps formed during the growth and cooling of a high purity FZ-^{28}Si crystal were investigated. The concentration of the carrier traps varies in the ingot but is below $10^{12}\,\mathrm{cm}^{-3}$. From the electrical and PL measurements, the P dopant concentration reaches $6 \times 10^{13}\,\mathrm{cm}^{-3}$ in the tail part of the ingot and is $<10^{13}\,\mathrm{cm}^{-3}$ in the top part. The obtained shallow trap parameters and the correlation of their concentrations with the P donor concentration supports the proposed identification of the detected traps as small interstitial clusters. The deep trap most probably is related to back-gliding dislocations appeared in the tail part of the crystal during post growth crystal cooling at $T > 850\,^{\circ}$C.

Acknowledgements We thank H. Bettin and P. Becker for helpful discussions and the 'Kg2' project of the PTB for the generous supply of the ^{28}Si samples.

References

[1] M. Steger, K. Saeedi, M. L. W. Thewalt, J. J. L. Morton, H. Riemann, N. V. Abrosimov, P. Becker, and H.-J. Pohl, Science **336**, 1280 (2012).
[2] P. Becker, H.-J. Pohl, H. Riemann, and N. V. Abrosimov, Phys. Status Solidi A **207**, 49 (2010).
[3] D. P. Franke, M. Szech, F. M. Hrubesch, H. Riemann, N. V. Abrosimov, P. Becker, H.-J. Pohl, K. M. Itoh, M. L. W. Thewalt, and M. S. Brandt, Phys. Rev. B **94**, 235201 (2016).
[4] M. Steger, A. Yang, D. Karaiskaj, M. L. W. Thewalt, E. E. Haller, J. W. Ager, M. Cardona, H. Riemann, N. V. Abrosimov, A. V. Gusev, A. D. Bulanov, A. K. Kaliteevskii, O. N. Godisov, P. Becker, and H.-J. Pohl, Phys. Rev. B **79**, 205210 (2009).
[5] M. Steger, A. Yang, T. Sekiguchi, K. Saeedi, M. L. W. Thewalt, M. O. Henry, K. Johnston, H. Riemann, N. V. Abrosimov, M. F. Churbanov, A. V. Gusev, A. K. Kaliteevskii, O. N. Godisov, P. Becker, and H.-J. Pohl, J. Appl. Phys. **110**, 081301 (2011).
[6] G. L. Miller, D. V. Lang, and L. C. Kimerling, Annu. Rev. Mater. Sci. **7**, 377 (1977).
[7] L. Dobaczewski, A. R. Peaker, and K. Bonde Nielsen, J. Appl. Phys. **96**, 4689 (2004).
[8] M. Allardt, Vl. Kolkovsky, K. Irmscher, and J. Weber, J. Appl. Phys. **112**, 103701 (2012).
[9] M. Tajima, Appl. Phys. Lett. **32**, 719 (1978).
[10] K. L. Schumacher and R. L. Whitney, J. Electron. Mater. **18**, 681 (1989).
[11] A. A. Istratov, H. Hieslmair, C. Flink, and E. R. Weber, Rev. Sci. Instrum. **69**, 244 (1998).
[12] V. V. Kveder, Yu. A. Osipyan, W. Schröter, and G. Zoth, Phys. Status Solidi A **72**, 701 (1982).
[13] P. Omling, E. R. Weber, L. Montelius, H. Alexander, and J. Michel, Phys. Rev. B **32**, 6571 (1985).
[14] Y. Tokumaru, H. Okushi, T. Masui, and T. Abe, Jpn. J. Appl. Phys. 2, **21**, L443 (1982).
[15] S. D. Brotherton and P. Bradley, J. Appl. Phys. **53**, 5720 (1982).

[16] T. Mchedlidze, T. Arguirov, G. Jia, and M. Kittler, Phys. Status Solidi A **204**, 2229 (2007).
[17] D. Kot, T. Mchedlidze, G. Kissinger, and W. von Ammon, ECS J. Solid State Sci. Technol. **2**, P9 (2013).
[18] http://www.laplacedlts.eu/defectTV/
[19] T. Mchedlidze and M. Suesawa, Phys. Rev. B **70**, 205203 (2004).
[20] M. A. Khorosheva, V. V. Kveder, and M. Seibt, Phys. Status Solidi A **212**, 1695 (2015).
[21] A. Mühlbauer, A. Muiznieks, and J. Virbulis, J. Cryst. Growth **180**, 372 (1977).
[22] V. Voronkov and R. Falster, Mat. Sci. Eng. B **114**, 130 (2004).
[23] B. Park, G. Seo, and G. Kim, J. Cryst. Growth **222**, 74 (2001).